

Article

Proposal of a Reflector-Enhanced Solar Still Concept and Its Comparison with Conventional Solar Stills

Mehdi Soltanian ¹, Siamak Hoseinzadeh ^{2,*} and Davide Astiaso Garcia ²

¹ Graduate Faculty of Environment, College of Engineering, University of Tehran, Tehran 1417853111, Iran; mehdisoltanian@ut.ac.ir

² Department of Planning, Design, and Technology of Architecture, Sapienza University of Rome, 00185 Rome, Italy; davide.astiasogarcia@uniroma1.it

* Correspondence: siamak.hosseinzadeh@uniroma1.it

Abstract: Water scarcity is a global concern and poses significant problems to countries with arid and semi-arid climates, like Iran. Considering financial difficulties, a lack of knowledge about high-tech alternatives, low incomes, a lack of access to high-tech tools, and low maintenance capabilities in developing countries, solar still desalination is a decent technology for providing proper water, especially for rural areas. However, the low water-production rate using this method dictates a very vast area requirement for solar still farms in order to provide significant amounts of water. In this research, we proposed a mirror-enhanced solar still and mathematically compared its water-production rate to that of conventional ones. In comparison to conventional solar stills, our proposed reflector-enhanced solar still benefits from several improvements, including lower glass temperatures, increased water basing temperatures, and receiving much more solar irradiation. Hence, the proposed system can increase water production from 7.5 L/day to 24 L/day. The results showed that the proposed method is highly effective and could be used in field-scale projects in arid and semi-arid climates.

Keywords: desalination; distilled water machine; enhanced solar still; solar cooker; sustainable development



Citation: Soltanian, M.; Hoseinzadeh, S.; Astiaso Garcia, D. Proposal of a Reflector-Enhanced Solar Still Concept and Its Comparison with Conventional Solar Stills. *Water* **2024**, *16*, 355. <https://doi.org/10.3390/w16020355>

Academic Editor: Constantinos V. Chrysikopoulos

Received: 26 December 2023

Revised: 10 January 2024

Accepted: 16 January 2024

Published: 21 January 2024



Copyright: © 2024 by the authors. Licensee MDPI, Basel, Switzerland. This article is an open access article distributed under the terms and conditions of the Creative Commons Attribution (CC BY) license (<https://creativecommons.org/licenses/by/4.0/>).

1. Introduction

Although the earth is predominantly covered by water, in numerous nations across the globe, there is a notable and concerning trend of diminishing freshwater availability. The reduction in fresh water supply is facilitated by a confluence of factors; in particular, the escalation of the population, the unsustainable exploitation of groundwater resources, the infrequency of precipitation events [1], and the exponential growth of global industries have led to a substantial surge in the need for freshwater [2]. Moreover, approximately 80% of the global population resides in countries characterized by arid and semi-arid conditions [3]. Therefore, water scarcity, which means a lack of water supply or safe water quality, could be considered a widespread problem that causes competition for water. Currently, almost half of the earth's population is experiencing its consequences [4]. Considering irrigation activity has almost a 75% share of typical water usage [5], it is predictable that farmers and people living in agricultural areas will be some of the most-affected people by water scarcity, and research also shows almost 3.0 billion people in agricultural areas are experiencing a high water shortage [6–8]. To address the water shortage issue and align with SDGs, developing highly efficient mechanisms that require low maintenance and could provide proper water is of great importance [9–12].

In addition, energy is seen as a pivotal concern in the economic advancement of countries [13], and on a yearly basis, energy consumption in developing countries grows by 5% on average [14]. Consequently, renewable energy sources have garnered significant attention globally in recent years [15] and solar energy is the leading renewable energy source [16]; this is predicted to significantly impact energy security and environmental

problems in both emerging and established countries [17]. Solar power is the primary form of renewable energy utilized for generating electricity [18], operating solar collectors [19–21], cooking with solar energy [22,23], drying with solar energy [24], combining solar and biomass energy [24], and heating metals [24]. As a result, although desalination approaches like reverse osmosis [25], ion exchange [26], and other common desalination methods [27–30] have been used worldwide, the main possible drawbacks of these systems are their setup costs, operational costs, and high energy consumption, [31,32], which leads to a significant interest in utilizing user-friendly and eco-friendly techniques such as solar stills for the purpose of desalinating water [1]. The use of solar energy reduces the reliance on fossil fuels and toxic substances, resulting in decreased emissions of greenhouse gases that contribute to global warming [2].

Due to its enormous popularity, researchers have been endeavoring to develop an ideal system with a similar underlying mechanism and minor modifications by implementing design modifications or using various methods for economic optimization [33], such as thermoelectric methods [34]; mirrors [35]; heat pipes [36]; finned plates [37]; surface coatings [38]; single and double slopes [39–41]; single, multiple, and stepped basins [42–46]; and pyramid and spherical methods [47,48]. Jeevadason and Padmini [49] examined the effects of using a novel glass cover design and found that it resulted in a 51.5% increase in water productivity. Mevada et al. [50] examined the impact of various energy storage materials, such as black granite and marble stone, on water productivity and the rate of evaporation enhancement. Ghani Hameed [51] achieved a 40% improvement in water generation compared to standard methods by employing fins and a glass cooling approach. Panchal et al. [52] employed an evacuated tube collector and hollow bumps to enhance the efficiency of desalination. The redesigned solar still yielded 2.44 times the amount of water compared to the traditional solar still. Abdullah et al. [53] conducted an evaluation of the impact of nano-PCM, a heating element, and finned absorbers on the production of water in solar stills. The findings showed a significant improvement of 166% in the water output compared to that using conventional methods. Gupta et al. [54] conducted research to quantify the enhanced efficiency of solar distillation, an increase of 10.6%, compared to PV/T-FPC solar desalination. Xiao et al. [55] integrated PV/thermal technology with solar distillation to enhance the efficiency of the device. They found that the temperature of the saline water increased by 16.4% and the daily production of the system increased by 51.7%. In a study conducted by Kumar and Tiwari [56], the impact of photovoltaic systems on sun still (SS) efficiency was examined. The study found that the production of the conventional system was almost 2250 mL, whereas the production of modified solar desalination was 7220 mL.

The authors assert that the improvement of solar stills employing traditional materials, which can be maintained without the need for specialized skill, is of high importance, especially for privileged rural areas in developing countries and in arid climates, like rural areas in the south of Iran, which is not only facing a lack of groundwater, but its high TDS also makes it undesirable for domestic and agricultural usage. In this regard, we proposed a parabolic solar collector solar still (PSCSS) desalination system. The proposed system is a combination of a parabolic solar cooker idea and a solar still that greatly increases the input solar energy into the solar still and significantly enhances the evaporation and water-production rates. In addition, in this system, a new pathway for water was considered, which reduces the glass temperature while increasing the water temperature before feeding into the basin of the solar still. This method can increase the water temperature in the system and improve the evaporation rate. In this research, the design and evaluation of the water-production capacity of the proposed PSCSS were conducted and compared to those in a conventional solar still system.

To estimate the solar irradiation incident on the parabolic disc, we utilized the annual mean value of the sun irradiation in the south of Iran based on the data available on the World Bank website [57], which are presented in Figure 1. In order to streamline the

calculations, we divided the total annual energy by 365 and assumed that the distribution of light radiation during a day follows a triangle pattern with a duration of 12 h.

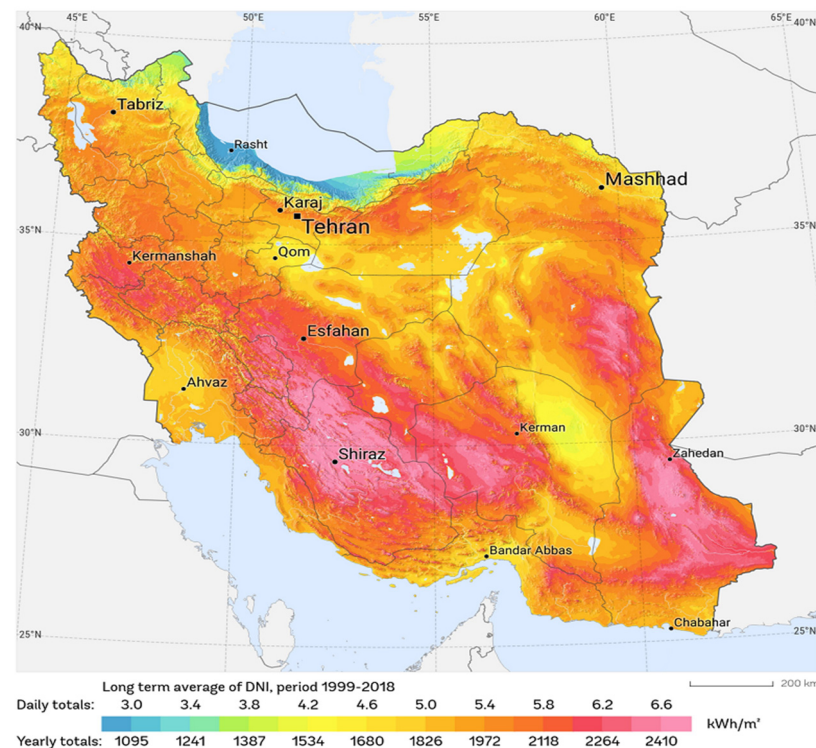


Figure 1. Solar irradiation of Iran [57].

2. The Fundamental Working of Solar Stills

An essential solar distiller consists of a reservoir containing a shallow layer of saline water in a basin that is colored black, a glass in an inclined position, a channel for collecting fresh water, a thermal barrier on all sides except for the glass one, an exit valve for removing solid sediments from the basin, and an inlet for introducing water. The storage container is filled with natural light, which heats the saline water within the basin, which then vaporizes. The vapors condense into liquid water upon the passage of heat to the glass cover. Condensed drops from the tilting lid are collected in the extraction canal located on the side wall of the still. The salts and pollutants are left behind and can be removed using the removal process. Although solar stills have the ability to transform salt water into low-TDS water, they are not efficient and have a limited capacity for water production [58].

3. Climate of Iran

With an area of 1,648,000 km² and a population of more than 80 million in 2017, Iran is the seventeenth biggest country in the world and is located in the western region of Asia [59,60]. Agricultural land makes up nearly 11.2% of the country's total land area, while 8.7% is forested, 19.7% is arid land, and 7.3% is industrial/residential. In recent years, the nation has seen a decline in precipitation and is faced with drought and shortages of water [61]. The climate in Iran is predominantly arid and semi-arid, with the exception of the mountainous regions in the northern and western parts of the entire country. In addition, apart from the coastal regions, the temperature in Iran exhibits a substantial annual variation, ranging from approximately 22 °C to 26 °C. The majority of Iran experiences the influence of subtropical high air masses throughout the summer season. These result in the occurrence of scorching summers in the country, while precipitation reduces to 100 mm or less in the central and eastern regions of Iran. Iran has a favorable geographical location for receiving solar energy. The sun irradiation in Iran is predicted to be around 1800 to 2200 kWh/m² per year, which exceeds the global average. Iran has a

high average annual number of over 280 sunny days, which covers over ninety percent of its territory and represents a significant and lucrative energy resource [62].

4. Mathematical Calculation

4.1. Energy Analysis

One method for determining the energy efficiency of a system is to calculate the ratio of the system’s productivity to the total quantity of energy that it absorbs from solar radiation. The equation below shows how energy efficiency could be measured effectively [1,63].

$$\eta_{daily} = \frac{m_{ev} \times h_{fg}}{I_t \times A_b} \tag{1}$$

The variables I_t (W/m^2), m_{ev} (L/h), and h_{fg} represent the cumulative daily radiation, the daily production of the system, and the latent heat of vaporization, respectively. Furthermore, A_b represents the precise measurement of the surface area of the absorber in a traditional solar desalination setup. In a simple system, A_b is equal to the basin of the solar still, which in this study is 1 m^2 , and in our proposed modified system, A_b refers to the combined area of both the reflector plate and the absorber plate in a solar still.

4.2. Thermal Equations

The heat transfer modes using energy balances and possible heat transfer routes in our proposed system are presented in Figure 2. The calculation of the volume of water production and the required area was conducted using Microsoft Excel 2020 by considering energy balance equations for the glass, water, and basin and for the parameters mentioned in Table 1 [64]. The energy balance equations are as follows:

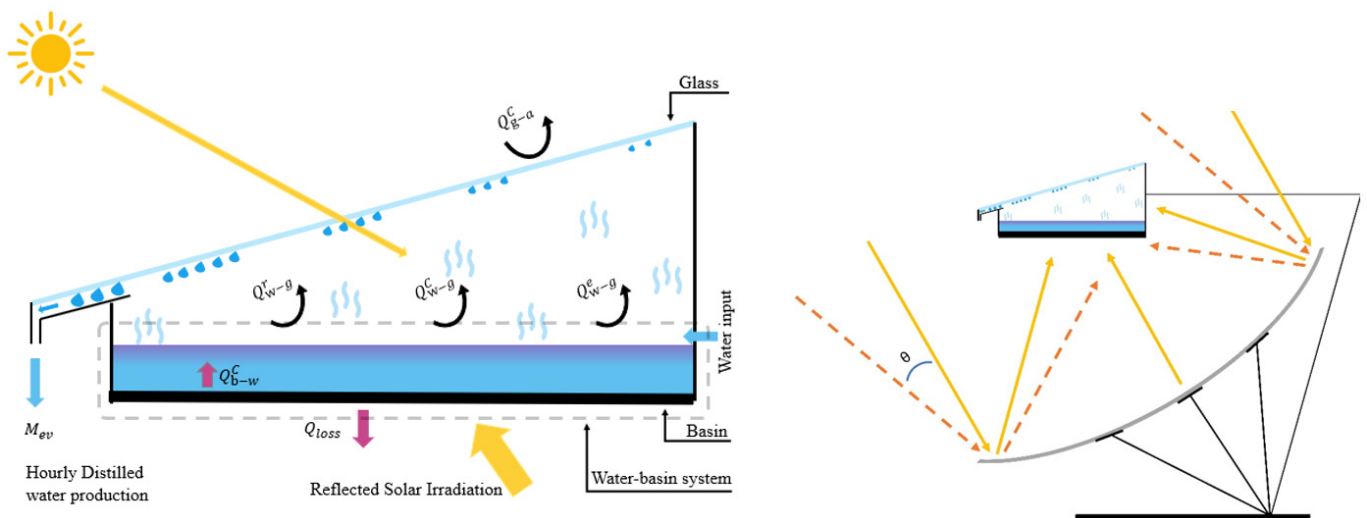


Figure 2. Schematic diagram of the energy balance of a single solar still slope and structure of the proposed system.

Table 1. Numerical parameters [54].

Parameter	Value	Parameter	Value	Parameter	Value
ρ_g	2500 ($kg\ m^{-3}$)	ρ_b	7800 ($kg\ m^{-3}$)	Water thickness	1 cm
Cp_g	840 ($J\ kg^{-1}\ K^{-1}$)	Cp_b	460 ($J\ kg^{-1}\ K^{-1}$)	Insolation thickness	5 cm
Glass thickness	4 mm	Basin thickness	2 mm	Isolation K_i	0.059
α_g (irradiation sorption)	0.05	α_w (irradiation sorption)	0.05	α_b	0.9
τ_g (irradiation passing)	0.9	τ_w (irradiation passing)	0.95	A_b (area of the basin)	m^2

The energy balance of the glass cover [45]:

$$M_g C p_g \frac{dT_g}{dt} = Q_{w-g}^c + Q_{w-g}^r + Q_{w-g}^e - Q_{g-a}^c - Q_{g-s}^r + \alpha_g A_g I(t) \tag{2}$$

In this equation and on the left side, M_g , $C p_g$, and T_g are the mass of glass, the specific heat transfer, and the glass temperature. On the right side of the equation, α_g , A_g , and $I(t)$ are the sorption percentage, the area of the glass, and sun irradiation, respectively. In addition, Q_{w-g}^c , Q_{w-g}^r , Q_{w-g}^e , Q_{g-a}^c , and Q_{g-s}^r are the convection energy input from the water to the glass, the radiant energy input from the water to the glass, the evaporation energy input from the water to the glass, the convective energy loss from the glass to the air, and the radiant energy loss from the glass to the sky.

The energy balance for the water [45]:

$$M_w C p_w \frac{dT_w}{dt} = Q_{b-w}^c - Q_{w-g}^c - Q_{w-g}^r - Q_{w-g}^e - Q_{fw} + \alpha_w \tau_g A_w I(t) \tag{3}$$

Similar to the above equation, this equation is written for the water’s energy balance, and the differences from the previous equation are Q_{fw} , τ_g , and A_w , which are related to the loss of energy because of water production and saltwater entering the basin, the percentage of solar irradiation that passed the glass, and the area of the water in the basin.

The energy balance for the basin [45]:

$$M_b C p_b \frac{dT_w}{dt} = -Q_{b-w}^c - Q_{loss} + \alpha_b \tau_w \tau_g A_b I(t) + Q_{R-b}^r \tag{4}$$

where A_w , A_b , T_w , and T_g are the area of water, the basin area, the temperature of the water, and the temperature of the glass, respectively. In addition, $-Q_{loss}$, Q_{R-b}^r , τ_w , and A_b are the loss of energy from the basin to the air, the irradiation energy from the reflector to the basin, the solar irradiation that passed the water depth, and the basin area.

The convection heat transfer between the water and the glass can be calculated as [65]

$$Q_{w-g}^c = h_{w-g}^c A_w (T_w - T_g) \tag{5}$$

The radiation heat transfer between the water and the glass can be calculated as

$$Q_{w-g}^r = h_{w-g}^r (T_w - T_g) \tag{6}$$

The evaporation heat transfer between the water and the glass can be calculated as [65]

$$Q_{w-g}^e = h_{w-g}^e A_w (T_w - T_g) \tag{7}$$

The convection heat transfer between the basin and the water can be calculated as [66]

$$Q_{b-w}^c = h_{b-w}^c A_b (T_b - T_w) \tag{8}$$

In the mentioned equations, h_{w-g}^c , h_{w-g}^r , h_{w-g}^e , and h_{b-w}^c are the heat transfer coefficient of convection between the water and the glass, the radiation between the water and the glass, the evaporation between the water and the glass, and the convection between the basin and the water, respectively. The parameters that are used in the above equations can be calculated as below [65,67,68]:

$$h_{w-g}^e = 0.016237 \times h_{w-g}^c \times \frac{(P_w - P_g)}{T_w - T_g} \tag{9}$$

$$h_{fg} = (2401.67 - (2.389 \times T_w)) \times 10^3 \tag{10}$$

$$h_{w-g}^c = 0.884 \times \left[T_w - T_g + \frac{(P_w - P_g) \times (T_w + 273.15)}{268900 - P_w} \right]^{\frac{1}{3}} \quad (11)$$

$$P_w = \exp \left[25.314 - \left(\frac{5144}{T_w + 273} \right) \right] \quad (12)$$

$$P_g = \exp \left[25.314 - \left(\frac{5144}{T_g + 273} \right) \right] \quad (13)$$

P_w and P_g are the partial saturated vapor pressure in water and the glass temperature, respectively [67].

$$h_{w-g}^r = \varepsilon_{eff} \times \sigma \times \frac{(T_w + 237.15)^4 - (T_g + 237.15)^4}{T_w - T_g} \quad (14)$$

$$\varepsilon_{eff} = \left(\frac{1}{\varepsilon_w} + \frac{1}{\varepsilon_g} - 1 \right)^{-1} \quad (15)$$

$$h_{w-g}^e = 16.273 \times 10^{-3} \times h_{w-g}^c \left[\frac{P_w - P_g}{T_w - T_g} \right] \quad (16)$$

The solar irradiation reflected from a reflector to the basin of the solar still:

$$Q_{R-b}^r = A_b \times h_{r-b} \times irradiation$$

The hourly water production of the solar still [69]:

$$m_{ev} = \frac{h_{w-g}^e (T_w - T_g) \times 3600}{h_{fg}} \quad (17)$$

where m_{ev} and h_{fg} are the hourly water production (liter/hour) and the latent heat of evaporation ($W/m^2 K$). To facilitate the calculation and by considering the equal temperatures of the basin and the water, which is almost a correct assumption, Equations (2) and (3) can be combined, and Equation (18) will be extracted. In this research, we utilized this equation. So, as shown in Figure 4, we consider the water and the basin a system, and we consider the input and output energy to this system.

$$M_w C p_w \frac{dT_w}{dt} + M_b C p_b \frac{dT_w}{dt} = -Q_{w-g}^c - Q_{w-g}^r - Q_{w-g}^e - Q_{fw} - Q_{loss} + \alpha_b \tau_w \tau_g A_b I(t) + \alpha_w \tau_g A_w I(t) \quad (18)$$

5. Description of the Proposed System

According to the climatic conditions of the study area and previous studies in south Iran, despite the initial high cost, the use of solar energy is a good option for a long period of time. In addition, previous research shows that the water-production rate of solar desalination systems is almost $0.5 L/m^2$ hr. Therefore, it does not seem reasonable to use conventional solar stills unless utilizing a modifications approach, which is capable of significantly reducing the required area. As a result, in this research, an effort was made to provide the water with the minimum required number of modified solar still systems with no high-tech materials.

The mathematical inquiry involves two solar stills that have identical features. One of the solar stills is equipped with a parabolic solar collector to function as an improved solar still, while the other one remains a traditional solar still for the sake of comparison. The solar stills consist of a galvanized steel sheet that is 0.002 m thick and has an effective basin area of $1 m^2$. The object consists of a black basin that is tightly sealed at the top with a transparent glass cover. The upper glass layer is 4 mm thick and is inclined at a 30-degree angle relative to the horizontal surface. The calculation is performed assuming no leakage. Furthermore, the orientation of both systems is deemed comparable. The water

temperature increases due to sun radiation, facilitated by convective heat transfer from the water to the basin. The water vapor ascends, departs from the surface of the basin, encounters a barrier, and results in the condensation of vapors to water.

The main drawbacks of conventional solar still systems are the high required energy for heating the water, the elevated temperature of the glass during the working time, and the limited working time. As shown in Figure 3, in order to overcome the high temperature of the glass, a new water pathway for the solar still system was used in this research. In the proposed new system, the water entrance pathway was changed, and after passing through the grooves of the top glass, the heated water feeds into the basin.

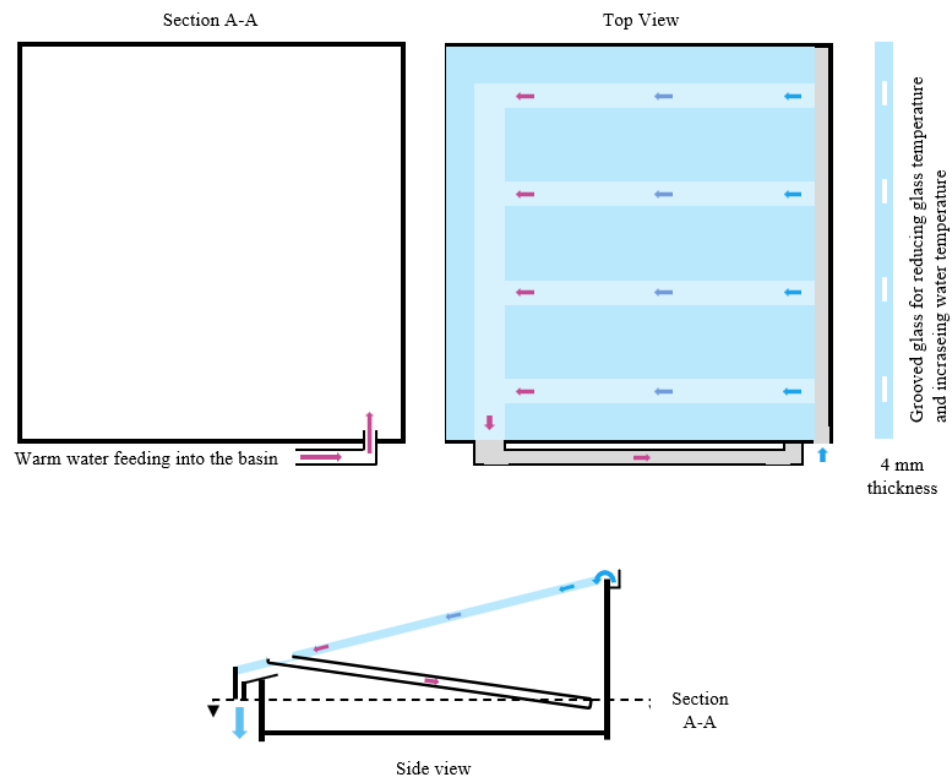


Figure 3. Describing new pathway of water.

In order to make the calculations simpler, instead of using the exact radiation values, we assumed that the hourly solar radiation distribution is geometrical. Therefore, as shown in Figure 4, we assumed that the daylight period is 12 h of radiation, and its distribution is linear. Although this assumption is not accurate, it is not far from the actual irradiation of the south of Iran. Based on the below calculation and Figure 4, it can be seen that approximately 0.55% of solar radiation is in the middle 4 h of the day, which justifies the 4 h period that we considered in this research. And the highest amount of water production is in the same hourly range.

$$\text{Entire area underline} = 0.5 \times 1000 \times [(18 - 6) + (13 - 11)] = 7000 \text{ Watt per day}$$

$$\text{Upper hatched area} = 0.5 \times 200 \times [(14 - 10) + (13 - 11)] = 600 \text{ Watt per day}$$

$$\text{Lower hatched area} = (14 - 10) \times 800 = 3200 \text{ Watt per day}$$

$$\text{Proportion of hatched area} : \frac{(3200 + 600)}{7000} \times 100 \cong 55\%$$

Proposed Solar Energy Collection

Considering a parabolic reflector for improving solar energy systems is an appropriate approach [70], and as shown in Figure 2, the amount of radiation in the system can be increased to a great extent. However, the critical point is that the angle of the sun will be different during the day and during the year. Considering the angle of sun radiation in the south of Iran and based on Figure 5, it can be concluded that the solar radiation during a year is almost between 40 and 85 degrees.

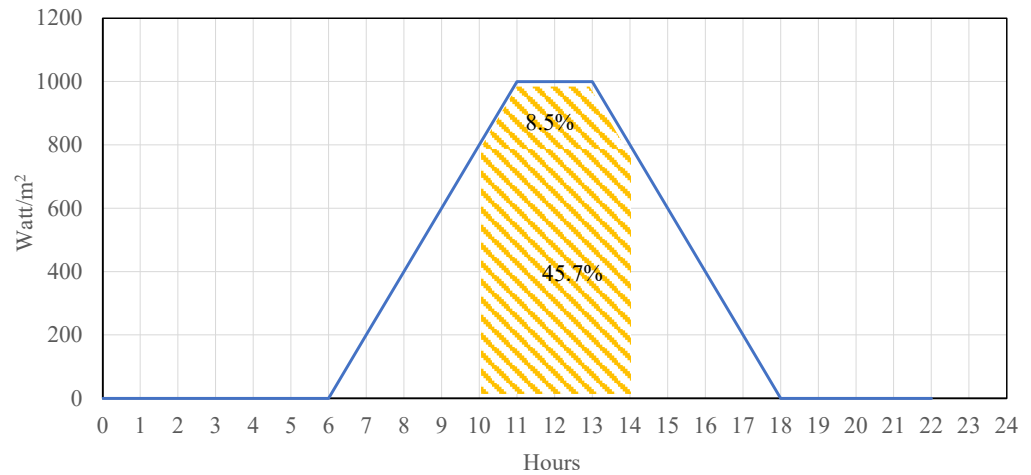


Figure 4. Linear approximation of solar irradiation in the south of Iran.

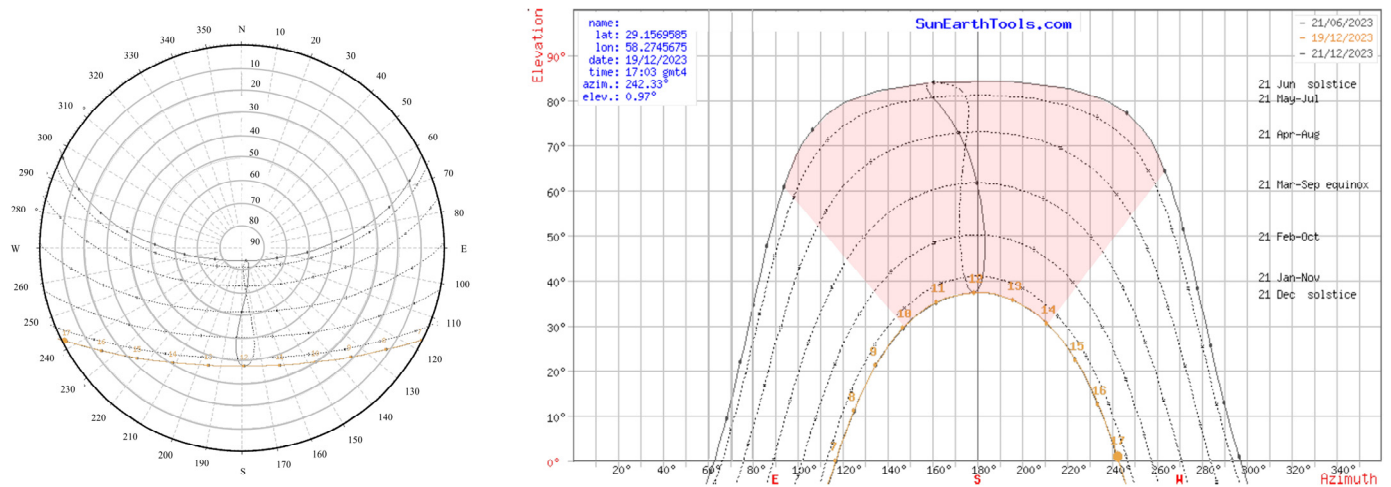


Figure 5. Solar irradiation angle in the south of Iran [71].

Since we are trying to propose a passive system that reflects solar radiation to the distillation system throughout the year without the need to apply direction changes or a solar radiation tracking system, the important point is to adjust the angle of the reflector in such a way that there is no need to change the angle of the reflector throughout the year and this system can reflect solar radiation to the solar still. This can be achieved by using the concept of a focal plane instead of the focal point of the reflector.

The radiation parallel to the main axis of the parabolic reflector focuses solar irradiation on the focal point; however, in such conditions and with the change in the angle of sun radiation during the day and throughout the year, the location of the focal point will be changed. Therefore, in order to limit the reflected energy from the parabolic reflector to the solar still, it is necessary to calculate the proportional theta angle based on the peak hours of solar radiation energy (middle 4 h of the day) and the dimensions of the distillation system in such a way that the stated objectives are met. As shown in Figure 6, according to

the target surface and the desired θ angle, the amount of surface needed for the reflector can be obtained [72]. Considering that the radiation angle in the desired geographical area is between 40 and 85 degrees, if the reflecting direction is set in the middle of the two, the angle will become about 64 degrees, and the θ angle is 24 degrees. So, we can reflect the sun's radiation to the target surface (the bottom of the solar still system) all year round for at least 4 h a day.

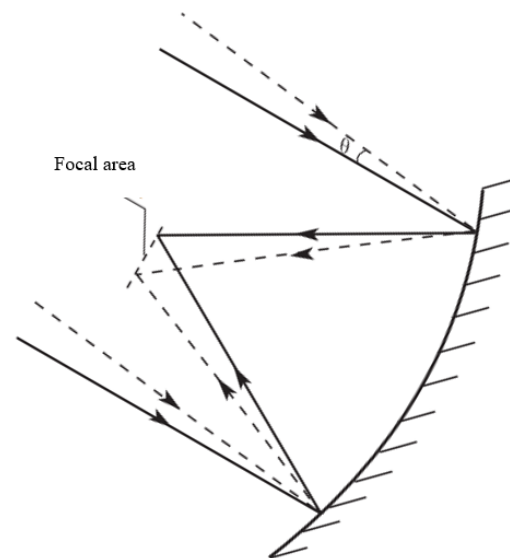


Figure 6. Definition of focal area concept [72].

As we know, every hour the movement of the sun is equivalent to 15 degrees. Therefore, it is necessary to consider a horizontal θ angle of 30 degrees so that the sun's radiation in the range of 2 h before and 2 h after noon can be reflected to the target area, that is, the bottom of the solar still system. Therefore, the previous calculated angle (24 degrees) is not proper for this purpose, and we considered the θ angle equal to 30 degrees and calculated the required reflective surface. As a result, based on the below equations [73], the reflector must have a surface four times higher than the target surface, which has a surface of 1 square meter.

$$C_{ideal} = \frac{1}{(\sin\Theta)^2} \quad (19)$$

$$C = \frac{A_{reflector}}{A_{target}} \quad (20)$$

This value means 4 square meters of reflecting surface, which results in a reflecting radius of 110 cm. Therefore, the parabolic reflector has an approximate radius of 110 cm and an angle direction of 63 degrees.

6. Mathematical Model Verification

In order to ensure the applicability and reliability of the results, validation of the utilized mathematical models is of great importance. In this regard, the mathematical equations and input data, such as ambient temperature, radiation intensity, and area of the solar still, from previous research published by [74] were utilized to validate the calculation process. As Figure 7 shows, our calculations are accurate enough that the modeling, calculation, facilitating assumptions, and outcome results are considered correct.

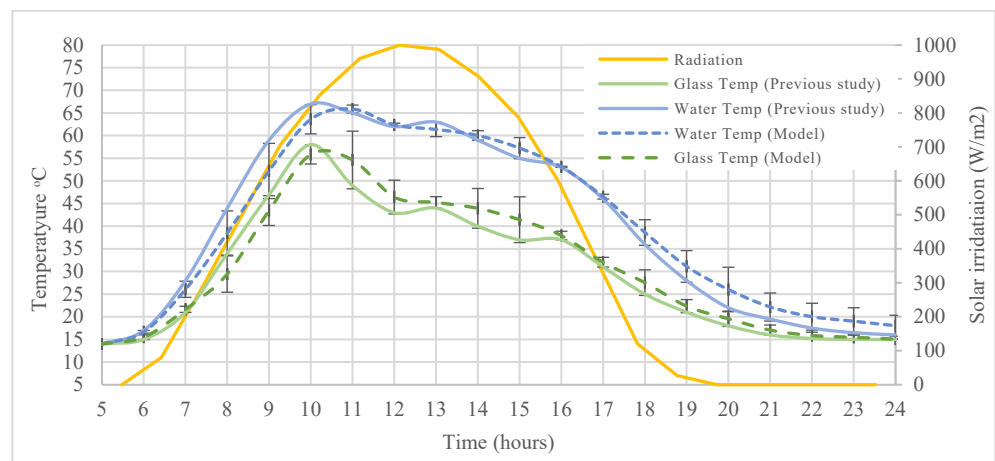


Figure 7. Model and calculation comparison with previously published research [74].

7. Results and Discussion

The south of Iran receives high solar irradiation and is sunny most of the year; therefore, a solar still farm is a good choice for providing the required water for irrigation. In this regard, the proposed system utilizes solar power as one of the mentioned enhancement mechanisms. Considering the effects of reflectors, Figure 8 presents the total solar energy that enters the solar still system. It is noteworthy that even when the focal area is not entirely on the basin, part of the reflection affects the energy entrance of the basin. Still, we ignore these energy inputs and consider the reflected solar radiation for 4 h.

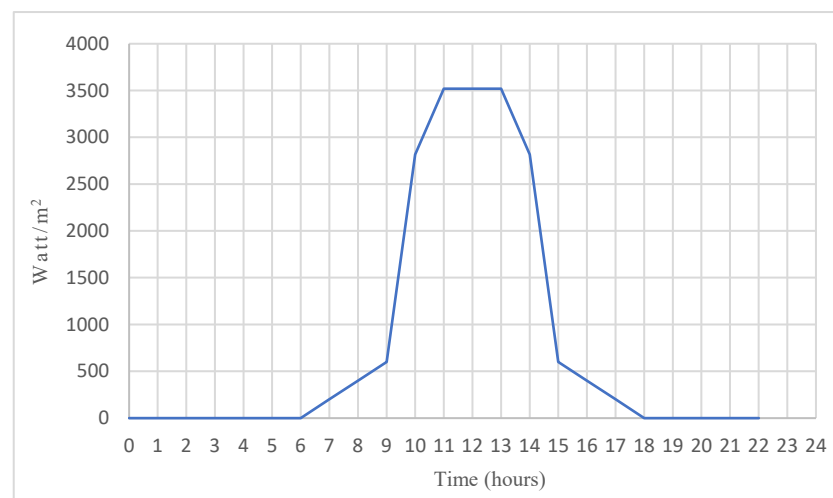


Figure 8. The solar energy input to the basin of the solar still considering the reflection.

The results presented are for a clear and sunny day despite the fact that solar intensity can vary from what we consider during a year. We consider a comparison between the proposed method and a conventional solar still calculated for summer, in which the solar radiation is high. As is presented in Figure 8, the maximum solar radiation was about 3520 W/m² and 2816 W/m² at noon and two hours before and after that, respectively. Figure 9 depicts the variation in temperature in the conventional and proposed systems. It is widely recognized that the disparity between the water and the glass cover inlet gives rise to an augmentation in the heat transfer through natural convection within the confines of the desalination system. The average difference between T_w and T_g in the conventional system was 6 °C. The highest T_g and T_w values were obtained at 1 p.m., about 58 °C and 67 °C, respectively, which led to a 34 °C temperature differential between the glass and the ambient temperature. The temperature fluctuation of the suggested system is also depicted

in Figure 9. The patterns exhibited similarities to conventional ones, albeit with significantly greater values, primarily attributed to the integration of a solar collector. Throughout the testing, the average temperatures of the basin, water, and glass cover were recorded as 48, 39 and 29 °C, respectively. The water production of solar desalination increased by widening the temperature difference between the temperature of the water (T_w) and the temperature of the condenser (T_g). The glass cover reached a maximum temperature of 88 °C at 2 p.m., while the water vapor reached a maximum temperature of 98 °C at the same time.

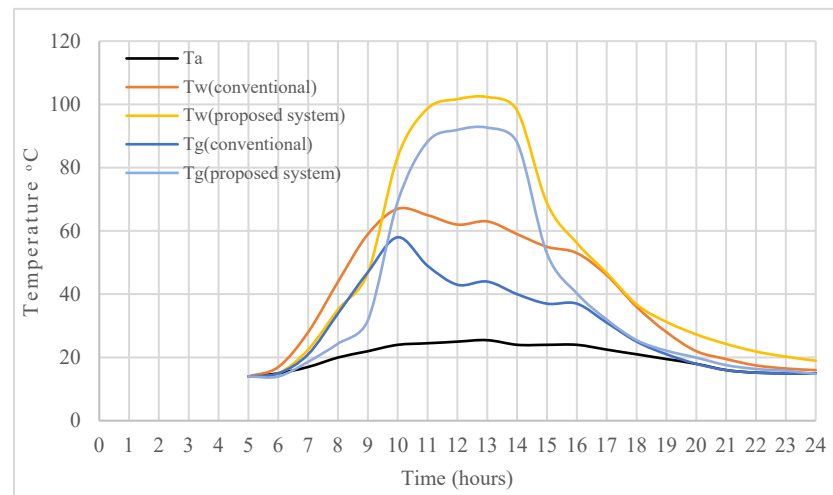


Figure 9. The temperature of the solar still systems.

Figure 10 illustrates the hourly fluctuation in freshwater production by both the traditional and proposed systems. The water generation trend is similar at different hours in both cases. The maximum hourly production, as determined, was 1.3 L/m² and 5.06 L/m², respectively, achieved at 1 p.m. The results demonstrated that the daily distillate production of the traditional and proposed methods was 23.29 L/m² and 7.73 L/m², respectively. The production increased by 301% compared to that of passive ones. The creation of water persisted in the evening after 6 p.m. even under low solar radiation in both. Furthermore, the amount of energy produced during the night in an active system was greater than in a passive system as a result of higher water and basin temperatures. The use of a solar collector increased the system's absorption area and enhanced the water temperature in the solar still system.

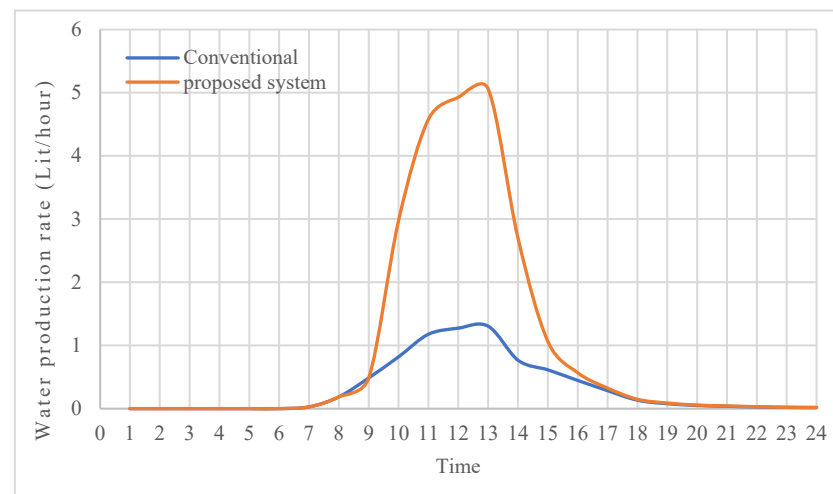


Figure 10. Cont.

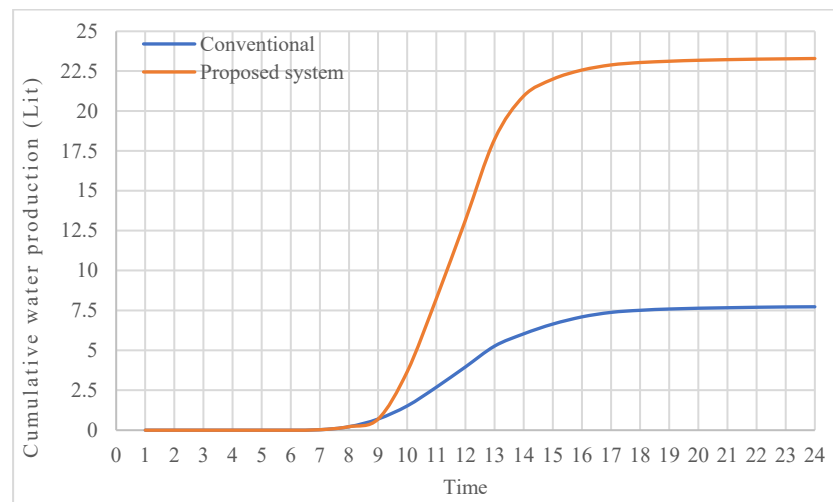


Figure 10. Water production and cumulative water production per day of the proposed system.

Figure 11 displays the hourly energy efficiency of the systems. The efficiency of the solar still paired with a solar collector was higher than that of a traditional system due to the increased absorption area of the device. It was noted that the suggested system exhibited higher energy efficiency compared to conventional methods during different hours of testing. This was attributed to the utilization of a solar reflector. The conventional mechanism achieved a maximum hourly energy efficiency of 67.9%, whereas the proposed system achieved a maximum hourly energy efficiency of 78.2%. The daily energy efficiency for the systems was 25.6% and 32.6%, respectively.

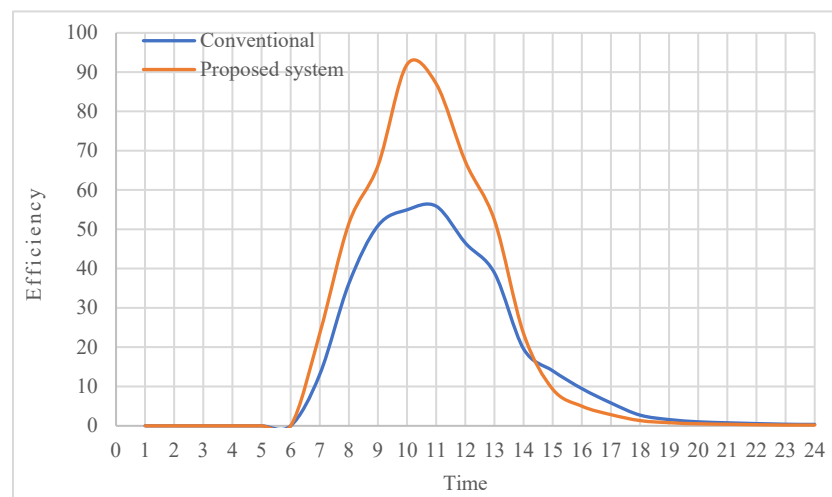


Figure 11. Energy efficiency of the systems.

8. Conclusions

Providing appropriate water in arid and semi-arid areas that are facing water shortages is of great importance, especially when agricultural activity is the leading financial resource of a local community. In the south of Iran, the local economy is highly dependent on agricultural activity, which is affected by high temperatures, high solar irradiation, a lack of proper water, and a lack of access to advanced technology. Although the presence of brackish wells near farms allows farmers to provide water for irrigation, high salinity and TDS dictate the need for a desalination system. Although there are a couple of studies trying to enhance the solar still water-production rate, they use high-tech elements like nonmaterial resources or combine the solar still system with other systems, which leads

to non-significant increases in the water-production rate. For instance, Ref. [53] used nanomaterials and phase exchange materials to enhance the water-production rate to 136%, which, although it is a significant enhancement, the more complicated structure using wicks and trays in addition to nanomaterials makes it difficult to build and, importantly, maintain this system in remote areas. In addition, photovoltaic-based systems, such what Xiao et al. [55] utilized to enhance the water productivity compared to the mirror system which was implemented in this research, are more vulnerable to environmental factors, like very high temperatures, severe wind, heavy rain, and freezing. Kabeel et al. [48], used a basic improvement in the basin by adding hollow fins to the basin of the solar still in order to improve the heat transfer from the basin to the water, which does not cause any particular problems in construction or maintenance. However, it could increase water production by 1.6 L, from 4 L to 5.6 L per day. In contrast, in this paper, a solar still is designed utilizing conventional solar still and solar cooking concepts to overcome the drawbacks mentioned in previous research. For this purpose, a parabolic reflector was used to significantly increase the solar energy input to the solar still system and improve the water-production rate. The results showed that using the proposed system can increase the daily water production from almost 7.5 L/day to almost 24 L/day, which can be highly applicable to field-scale projects of providing water for less privileged rural areas or farmers who are faced with high-TDS water sources. In addition, although the efficiency of the proposed system is higher than that of the conventional mechanism, the decreasing rate after noon is also higher, which illustrates the significant need to use methods to lower the energy loss of the system. This research illustrates the capability of solar still systems to integrate with other systems. For future research, the following information can be provided:

Parabolic Collector Design Optimization:

- Ensure that the parabolic collectors are specifically built to achieve the highest possible concentration of sunlight on the surface of the solar still.
- Investigate high-performance materials for constructing the parabolic collector in order to enhance its resilience and ability to reflect sun irradiation.
- Incorporation of Tracking devices:
- Deploy solar tracking devices for the parabolic collectors to accurately track the sun's trajectory throughout the day. This guarantees that the solar still receives the most favorable sunlight during the entire day, not just for 4 h.
- Selective Coating for Solar Steel:
- The coatings can be engineered to optimize absorption in the visible and near-infrared range while minimizing thermal energy dissipation through radiation.
- Environmental Considerations:
- Evaluate the ecological repercussions of the solar desalination system and strive for long-term viability. This may entail utilizing sustainable materials, implementing recycling techniques, and mitigating any adverse impacts on the local ecosystem.

Author Contributions: Conceptualization, M.S. and S.H.; Methodology, M.S. and S.H.; Software, M.S.; Validation, M.S.; Formal analysis, M.S., S.H. and D.A.G.; Investigation, M.S. and S.H.; Resources, S.H. and D.A.G.; Data curation, M.S. and S.H.; Writing—original draft, M.S. and S.H.; Writing—review & editing, S.H. and D.A.G.; Visualization, M.S. and S.H.; Supervision, S.H. and D.A.G.; Project administration, S.H. and D.A.G.; Funding acquisition, S.H. All authors have read and agreed to the published version of the manuscript.

Funding: This research received no external funding.

Data Availability Statement: Data are contained within the article.

Conflicts of Interest: The authors declare no conflicts of interest.

Nomenclature

Term	Description
HTC	Heat transfer coefficient
h_{w-g}^c	Convective HTC from seawater to glass, W per K per m ²
h_{w-g}^r	Radiative HTC from seawater to glass, W per K per m ²
h_{w-g}^e	Evaporative HTC from seawater to glass, W per K per m ²
Q_{w-g}^c	Rate of convective heat transfer within seawater and glass, W/m ²
Q_{w-g}^r	Rate of radiative heat transfer within seawater and glass, W/m ²
Q_{w-g}^e	Rate of evaporative heat transfer within seawater and glass, W/m ²
k_b	Basin thermal conductivity, W per m per °C
k_{ins}	Insulation thermal conductivity, W per m per °C
A	Surface area, m ²
c_p	Specific heat, J/kg °C
I_{sun}	Intensity of solar radiation, W/m ²
l_{ins}	Insulation thickness, m
l_b	Basin thickness, m
P_w	Partial saturated vapor pressure in seawater temperature, Pa
P_g	Partial saturated vapor pressure in glass temperature, Pa
T_w	Seawater temperature, °C
T_g	Glass temperature, °C
T_b	Basin temperature, °C
ρ	Density, kg/m ³
t	Time, s
σ	Stephan Boltzman, W/m ² °K ⁴
ε_{eff}	Emissivity

References

- Angappan, G.; Pandiaraj, S.; Alrubaie, A.J.; Muthusamy, S.; Said, Z.; Panchal, H.; Katekar, V.P.; Shoeibi, S.; Kabeel, A.E. Investigation on Solar Still with Integration of Solar Cooker to Enhance Productivity: Experimental, Exergy, and Economic Analysis. *J. Water Process Eng.* **2023**, *51*, 103470. [CrossRef]
- Abdullah, A.S.; Panchal, H.; Alawee, W.H.; Omara, Z.M. Methods Used to Improve Solar Still Performance with Generated Turbulence for Water Desalination- Detailed Review. *Results Eng.* **2023**, *19*, 101251. [CrossRef]
- Panchal, H.; Nurdianto, H.; Sadasivuni, K.K.; Hishan, S.S.; Essa, F.A.; Khalid, M.; Dharaskar, S.; Shanmugan, S. Experimental Investigation on the Yield of Solar Still Using Manganese Oxide Nanoparticles Coated Absorber. *Case Stud. Therm. Eng.* **2021**, *25*, 100905. [CrossRef]
- UNICEF Water and the Global Climate Crisis: 10 Things You Should Know. Available online: https://www.unicef.org/stories/water-and-climate-change-10-things-you-should-know?gclid=CjwKCAiAgeeqBhBAEiwAoDDhn_GhPkfm7QkiXzjceFMDu7CVPdMBZZHXKCe-ijTh5_uoSxGeCZ4_iBoCVykQAvD_BwE (accessed on 15 October 2023).
- United Nation Summary Progress Update 2021: SDG 6—Water and Sanitation for All. In *The UN-Water Integrated Monitoring Initiative*; UN-Water: Geneva, Switzerland, 2021; pp. 1–58.
- FAO Overcoming Water Challenges in Agriculture. Available online: <https://www.fao.org/state-of-food-agriculture/2020/en/> (accessed on 5 October 2023).
- Hosseini, K.; Nazeri Tahroudi, M. Annual and Seasonal Distribution Pattern of Rainfall in Iran and Neighboring Regions. *Arab. J. Geosci.* **2019**, *12*, 271. [CrossRef]
- Khani, S.M.R.; Bahadori, M.; Dehghani-Sanij, A. Experimental Investigation of a Modular Wind Tower in Hot and Dry Regions. *Energy Sustain. Dev.* **2017**, *39*, 21–28. [CrossRef]
- Omiddezyani, S.; Dehghani, Z.; Ahmadi, P.; Ashjaee, M.; Houshfar, E. Design and Optimization of an Integrated Novel Desalination System Based on the Temperature Difference between the Sea and Mountain. *Sol. Energy* **2023**, *258*, 37–56. [CrossRef]
- Soltani, M.; Moradi Kashkooli, F.; Dehghani-Sanij, A.R.; Nokhosteen, A.; Ahmadi-Joughi, A.; Gharali, K.; Mahbaz, S.B.; Dusseault, M.B. A Comprehensive Review of Geothermal Energy Evolution and Development. *Int. J. Green Energy* **2019**, *16*, 971–1009. [CrossRef]
- Dehghani-Sanij, A.R.; MacLachlan, S.; Naterer, G.F.; Muzychka, Y.S.; Haynes, R.D.; Enjilela, V. Multistage Cooling and Freezing of a Saline Spherical Water Droplet. *Int. J. Therm. Sci.* **2020**, *147*, 106095. [CrossRef]
- Abadi, M.M.; Izadi, I.; Jalili, B. Numerical Analysis of a Multi-Stage Evacuation Desalination in Tehran City. *Water Energy Int.* **2019**, *61*, 53–57.
- Karimi, H.; Adibhesami, M.A.; Bazazzadeh, H.; Movafagh, S. Green Buildings: Human-Centered and Energy Efficiency Optimization Strategies. *Energies* **2023**, *16*, 3681. [CrossRef]

14. Capellán-Pérez, I.; Campos-Celador, Á.; Terés-Zubiaga, J. Renewable Energy Cooperatives as an Instrument towards the Energy Transition in Spain. *Energy Policy* **2018**, *123*, 215–229. [[CrossRef](#)]
15. Dehghani-Sani, A.; Kashkooli, F.M. Special Issue: New Developments and Prospects in Clean and Renewable Energies. *Appl. Sci.* **2023**, *13*, 9632. [[CrossRef](#)]
16. Al Mallahi, M.N.; Assad, M.E.H.; Rejeb, O.; Delnava, H.; Asaad, S.; Tan, Y.C. A Review on Cleaning Techniques of Solar Photovoltaic Panels. *AIP Conf. Proc.* **2023**, *2847*, 40010. [[CrossRef](#)]
17. Bellos, E.; Tzivanidis, C. A Review of Concentrating Solar Thermal Collectors with and without Nanofluids. *J. Therm. Anal. Calorim.* **2019**, *135*, 763–786. [[CrossRef](#)]
18. Abdullah, A.S.; Alawee, W.H.; Mohammed, S.A.; Majdi, A.; Omara, Z.M.; Essa, F.A. Increasing the Productivity of Modified Cords Pyramid Solar Still Using Electric Heater and Various Wick Materials. *Process Saf. Environ. Prot.* **2023**, *169*, 169–176. [[CrossRef](#)]
19. Esmaeilion, F.; Soltani, M.; Hoseinzadeh, S.; Sohani, A.; Nathwani, J. Benefits of an Innovative Polygeneration System Integrated with Salinity Gradient Solar Pond and Desalination Unit. *Desalination* **2023**, *564*, 116803. [[CrossRef](#)]
20. Wheatley, G.; Rubel, R.I. Design Improvement of a Laboratory Prototype for Efficiency Evaluation of Solar Thermal Water Heating System Using Phase Change Material (PCMs). *Results Eng.* **2021**, *12*, 100301. [[CrossRef](#)]
21. Pambudi, N.A.; Nanda, I.R.; Saputro, A.D. The Energy Efficiency of a Modified V-Corrugated Zinc Collector on the Performance of Solar Water Heater (SWH). *Results Eng.* **2023**, *18*, 101174. [[CrossRef](#)]
22. Mawire, A.; Lentswe, K.; Owusu, P. Performance of Two Solar Cooking Storage Pots Using Parabolic Dish Solar Concentrators during Solar and Storage Cooking Periods with Different Heating Loads. *Results Eng.* **2022**, *13*, 100336. [[CrossRef](#)]
23. Verma, S.; Banerjee, S.; Das, R. A Fully Analytical Model of a Box Solar Cooker with Sensible Thermal Storage. *Sol. Energy* **2022**, *233*, 531–542. [[CrossRef](#)]
24. Krabch, H.; Tadili, R.; Idrissi, A. Design, Realization and Comparison of Three Passive Solar Dryers. Orange Drying Application for the Rabat Site (Morocco). *Results Eng.* **2022**, *15*, 100532. [[CrossRef](#)]
25. Kumar, H.A.; Venkateswaran, H.; Kabeel, A.E.; Chamkha, A.; Athikesavan, M.M.; Sathyamurthy, R.; Kasi, K. Recent Advancements, Technologies, and Developments in Inclined Solar Still—A Comprehensive Review. *Environ. Sci. Pollut. Res.* **2021**, *28*, 35346–35375. [[CrossRef](#)] [[PubMed](#)]
26. Naghipour, D.; Taghavi, K.; Jaafari, J.; Kabdashli, I.; Makkiabadi, M.; Javan Mahjoub Doust, M.; Javan Mahjoub Doust, F. Scallop Shell Coated Fe₂O₃ Nanocomposite as an Eco-Friendly Adsorbent for Tetracycline Removal. *Environ. Technol.* **2023**, *44*, 150–160. [[CrossRef](#)] [[PubMed](#)]
27. Keshavarzadeh, A.H.; Ahmadi, P.; Rosen, M.A. Technoeconomic and Environmental Optimization of a Solar Tower Integrated Energy System for Freshwater Production. *J. Clean. Prod.* **2020**, *270*, 121760. [[CrossRef](#)]
28. Liu, S.; Wang, Z.; Han, M.; Zhang, J. Embodied Water Consumption between Typical Desalination Projects: Reverse Osmosis versus Low-Temperature Multi-Effect Distillation. *J. Clean. Prod.* **2021**, *295*, 126340. [[CrossRef](#)]
29. Alirahmi, S.M.; Rahmani Dabbagh, S.; Ahmadi, P.; Wongwises, S. Multi-Objective Design Optimization of a Multi-Generation Energy System Based on Geothermal and Solar Energy. *Energy Convers. Manag.* **2020**, *205*, 112426. [[CrossRef](#)]
30. Al-Amshawee, S.; Yunus, M.Y.B.M.; Azoddein, A.A.M.; Hassell, D.G.; Dakhil, I.H.; Hasan, H.A. Electrodialysis Desalination for Water and Wastewater: A Review. *Chem. Eng. J.* **2020**, *380*, 122231. [[CrossRef](#)]
31. Cumo, F.; Astiaso Garcia, D.; Gugliermetti, F. Assessing the Potential Use of Solar Energy Source in Urban Areas Located in Natural Protected Sites. *Nat. Resour.* **2013**, *4*, 134–141. [[CrossRef](#)]
32. Do Thi, H.T.; Pasztor, T.; Fozer, D.; Manenti, F.; Toth, A.J. Comparison of Desalination Technologies Using Renewable Energy Sources with Life Cycle, PESTLE, and Multi-Criteria Decision Analyses. *Water* **2021**, *13*, 3023. [[CrossRef](#)]
33. Assareh, E.; Delpisheh, M.; Alirahmi, S.M.; Tafi, S.; Carvalho, M. Thermodynamic-Economic Optimization of a Solar-Powered Combined Energy System with Desalination for Electricity and Freshwater Production. *Smart Energy* **2022**, *5*, 100062. [[CrossRef](#)]
34. Shoeibi, S.; Kargarsharifabad, H.; Rahbar, N.; Khosravi, G.; Sharifpur, M. An Integrated Solar Desalination with Evacuated Tube Heat Pipe Solar Collector and New Wind Ventilator External Condenser. *Sustain. Energy Technol. Assess.* **2022**, *50*, 101857. [[CrossRef](#)]
35. Tanaka, H.; Nakatake, Y. A Simple and Highly Productive Solar Still: A Vertical Multiple-Effect Diffusion-Type Solar Still Coupled with a Flat-Plate Mirror. *Desalination* **2005**, *173*, 287–300. [[CrossRef](#)]
36. Shoeibi, S.; Rahbar, N.; Abedini Esfahlani, A.; Kargarsharifabad, H. Improving the Thermoelectric Solar Still Performance by Using Nanofluids—Experimental Study, Thermodynamic Modeling and Energy Matrices Analysis. *Sustain. Energy Technol. Assess.* **2021**, *47*, 101339. [[CrossRef](#)]
37. Shoeibi, S.; Kargarsharifabad, H.; Mirjalily, S.A.A.; Muhammad, T. Solar District Heating with Solar Desalination Using Energy Storage Material for Domestic Hot Water and Drinking Water—Environmental and Economic Analysis. *Sustain. Energy Technol. Assess.* **2022**, *49*, 101713. [[CrossRef](#)]
38. Sathyamurthy, R.; Ali, H.M.; Said, Z.; Kabeel, A.E.; El-Sebaey, M.S.; Gopalsamy, S.; Nagaraj, M.; Almasoud, N.; Alomar, T.S. Enhancing Solar Still Thermal Performance: The Role of Surface Coating and Thermal Energy Storage in Repurposed Soda Cans. *J. Energy Storage* **2024**, *77*, 109807. [[CrossRef](#)]
39. Hassan, H. Comparing the Performance of Passive and Active Double and Single Slope Solar Stills Incorporated with Parabolic Trough Collector via Energy, Exergy and Productivity. *Renew. Energy* **2020**, *148*, 437–450. [[CrossRef](#)]

40. Muthu Manokar, A.; Vimala, M.; Prince Winston, D.; Rajendran, D.R.; Sathyamurthy, R.; Kabeel, A.E. Year around Distilled Water Production, Energy, and Economic Analysis of Solar Stills—A Comparative Study. *Heat Transf.* **2020**, *49*, 3651–3662. [[CrossRef](#)]
41. Rubio, E.; Fernández, J.; Porta-Gándara, M. Modeling Thermal Asymmetries in Double Slope Solar Stills. *Renew. Energy* **2004**, *29*, 895–906. [[CrossRef](#)]
42. Zhang, L.; Xu, Z.; Bhatia, B.; Li, B.; Zhao, L.; Wang, E.N. Modeling and Performance Analysis of High-Efficiency Thermally-Localized Multistage Solar Stills. *Appl. Energy* **2020**, *266*, 114864. [[CrossRef](#)]
43. Seralathan, S.; Chenna Reddy, G.; Sathish, S.; Muthuram, A.; Dhanraj, J.A.; Lakshmaiy, N.; Velmurugan, K.; Sirisamphanwong, C.; Ngoenmeesri, R.; Sirisamphanwong, C. Performance and Exergy Analysis of an Inclined Solar Still with Baffle Arrangements. *Heliyon* **2023**, *9*, e14807. [[CrossRef](#)]
44. Baskaran, V.; Saravanane, R. Rendering Utility Water with Solar Still and Efficiency of Solar Stills with Different Geometry—A Review. *Environ. Nanotechnol. Monit. Manag.* **2021**, *16*, 100534. [[CrossRef](#)]
45. Kabeel, A.E.; Omara, Z.M.; Essa, F.A. Numerical Investigation of Modified Solar Still Using Nanofluids and External Condenser. *J. Taiwan Inst. Chem. Eng.* **2017**, *75*, 77–86. [[CrossRef](#)]
46. Nazari, S.; Daghigh, R. Techno-Enviro-Exergo-Economic and Water Hygiene Assessment of Non-Cover Box Solar Still Employing Parabolic Dish Concentrator and Thermoelectric Peltier Effect. *Process Saf. Environ. Prot.* **2022**, *162*, 566–582. [[CrossRef](#)]
47. Sadeghi, G.; Nazari, S. Retrofitting a Thermoelectric-Based Solar Still Integrated with an Evacuated Tube Collector Utilizing an Antibacterial-Magnetic Hybrid Nanofluid. *Desalination* **2021**, *500*, 114871. [[CrossRef](#)]
48. Kabeel, A.E.; El-Maghlany, W.; Abdelgaied, M.; Abdel-Aziz, M. Performance Enhancement of Pyramid-Shaped Solar Stills Using Hollow Circular Fins and Phase Change Materials. *J. Energy Storage* **2020**, *31*, 101610. [[CrossRef](#)]
49. Jeevadason, A.W.; Padmini, S. Experimental Investigation of a Passive Type Solar Still with Double Wedge Shape Glass Cover. *Mater. Today Proc.* **2022**, *56*, 308–313. [[CrossRef](#)]
50. Mevada, D.; Panchal, H.; Ahmadein, M.; Zayed, M.E.; Alsaleh, N.A.; Djuansjah, J.; Moustafa, E.B.; Elsheikh, A.H.; Sadasivuni, K.K. Investigation and Performance Analysis of Solar Still with Energy Storage Materials: An Energy- Exergy Efficiency Analysis. *Case Stud. Therm. Eng.* **2022**, *29*, 101687. [[CrossRef](#)]
51. Hameed, H.G. Experimentally Evaluating the Performance of Single Slope Solar Still with Glass Cover Cooling and Square Cross-Section Hollow Fins. *Case Stud. Therm. Eng.* **2022**, *40*, 102547. [[CrossRef](#)]
52. Panchal, H.; Sohani, A.; Van Nguyen, N.; Shoeibi, S.; Khiadani, M.; Huy, P.Q.; Hoseinzadeh, S.; Kabeel, A.E.; Shaik, S.; Cuce, E. Performance Evaluation of Using Evacuated Tubes Solar Collector, Perforated Fins, and Pebbles in a Solar Still—Experimental Study and CO₂ Mitigation Analysis. *Environ. Sci. Pollut. Res.* **2023**, *30*, 11769–11784. [[CrossRef](#)]
53. Abdullah, A.S.; Omara, Z.M.; Essa, F.A.; Alqsair, U.F.; Aljaghtam, M.; Mansir, I.B.; Shanmugan, S.; Alawee, W.H. Enhancing Trays Solar Still Performance Using Wick Finned Absorber, Nano- Enhanced PCM. *Alex. Eng. J.* **2022**, *61*, 12417–12430. [[CrossRef](#)]
54. Gupta, V.S.; Singh, D.B.; Mishra, R.K.; Sharma, S.K.; Tiwari, G.N. Development of Characteristic Equations for PVT-CPC Active Solar Distillation System. *Desalination* **2018**, *445*, 266–279. [[CrossRef](#)]
55. Xiao, L.; Shi, R.; Wu, S.-Y.; Chen, Z.-L. Performance Study on a Photovoltaic Thermal (PV/T) Stepped Solar Still with a Bottom Channel. *Desalination* **2019**, *471*, 114129. [[CrossRef](#)]
56. Kumar, S.; Tiwari, A. Design, Fabrication and Performance of a Hybrid Photovoltaic/Thermal (PV/T) Active Solar Still. *Energy Convers. Manag.* **2010**, *51*, 1219–1229. [[CrossRef](#)]
57. THE WORLD BANK Solar Irradiation and PV Power Potential Maps. Available online: <https://datacatalog.worldbank.org/search/dataset/0039610/Iran---Solar-irradiation-and-PV-power-potential-maps> (accessed on 22 November 2023).
58. Thomas-Hillman, I.; Laybourn, A.; Dodds, C.; Kingman, S.W. Realising the Environmental Benefits of Metal–Organic Frameworks: Recent Advances in Microwave Synthesis. *J. Mater. Chem. A* **2018**, *6*, 11564–11581. [[CrossRef](#)]
59. The World Bank. *World Bank Country and Lending Group*; The World Bank: Washington, DC, USA, 2023.
60. The World Bank. *Iran, Islamic, Rep*; The World Bank: Washington, DC, USA, 2023.
61. Mousavi, A.; Ardalan, A.; Takian, A.; Ostadtaghizadeh, A.; Naddafi, K.; Bavani, A.M. Climate Change and Health in Iran: A Narrative Review. *J. Environ. Health Sci. Eng.* **2020**, *18*, 367–378. [[CrossRef](#)] [[PubMed](#)]
62. Alamdari, P.; Nematollahi, O.; Alemrajabi, A.A. Solar Energy Potentials in Iran: A Review. *Renew. Sustain. Energy Rev.* **2013**, *21*, 778–788. [[CrossRef](#)]
63. Kabeel, A.E. Performance of Solar Still with a Concave Wick Evaporation Surface. *Energy* **2009**, *34*, 1504–1509. [[CrossRef](#)]
64. Tiwari, G.N.; Dimri, V.; Chel, A. Parametric Study of an Active and Passive Solar Distillation System: Energy and Exergy Analysis. *Desalination* **2009**, *242*, 1–18. [[CrossRef](#)]
65. Halima, H.; Frikha, N.; Ben Slama, R. Numerical Investigation of a Simple Solar Still Coupled to a Compression Heat Pump. *Desalination* **2014**, *337*, 60–66. [[CrossRef](#)]
66. Edalatpour, M.; Aryana, K.; Kianifar, A.; Tiwari, G.; Mahian, O.; Wongwises, S. Solar Stills: A Review of the Latest Developments in Numerical Simulations. *Sol. Energy* **2016**, *135*, 897–922. [[CrossRef](#)]
67. Aldoori, W.H.; Ahmed, A.H.; Ahmed, A.M. Performance Investigation of a Solar Water Distiller Integrated with a Parabolic Collector Using Fuzzy Technique. *Heat Transf. Res.* **2020**, *49*, 120–134. [[CrossRef](#)]
68. Arun Kumar, S.; Kumar, P.; Sathyamurthy, R.; Manokar, A. Experimental Investigation on Pyramid Solar Still with Single and Double Collector Cover-Comparative Study. *Heat Transf. Res.* **2019**, *49*, 103–119. [[CrossRef](#)]

69. Kalidasa Murugavel, K.; Sivakumar, S.; Ahamed, J.; Chockalingam, K.K.S.K.; Srithar, K. Single Basin Double Slope Solar Still with Minimum Basin Depth and Energy Storing Materials. *Appl. Energy* **2010**, *87*, 514–523. [[CrossRef](#)]
70. Mehrpooya, M.; Ghadimi, N.; Marefati, M.; Ghorbanian, S.A. Numerical Investigation of a New Combined Energy System Includes Parabolic Dish Solar Collector, Stirling Engine and Thermoelectric Device. *Int. J. Energy Res.* **2021**, *45*, 16436–16455. [[CrossRef](#)]
71. Sun Earth Tool Sun Earth Tool. Available online: <https://www.sunearthtools.com/> (accessed on 20 October 2023).
72. Zheng, H. Solar Energy Utilization and Its Collection Devices. In *Solar Energy Desalination Technology*; Elsevier: Amsterdam, The Netherlands, 2017; ISBN 9780128054116.
73. Ari, R. *Active Solar Collectors and Their Applications*; Oxford University Press: Oxford, UK, 1985; ISBN 0195035461/9780195035469.
74. Khadija, Z.; M'barek, F.; Hicham, M. Effect of Metal Oxide Nanofluids on the Performance of Passive Solar Still Single Slope for Two Different Absorbent Plates. *Heat Transf.* **2022**, *2*, 101320.

Disclaimer/Publisher's Note: The statements, opinions and data contained in all publications are solely those of the individual author(s) and contributor(s) and not of MDPI and/or the editor(s). MDPI and/or the editor(s) disclaim responsibility for any injury to people or property resulting from any ideas, methods, instructions or products referred to in the content.